MODELLING OF BRASS INSTRUMENT VALVES

Stefan Bilbao,

Acoustics and Fluid Dynamics Group/Music
University of Edinburgh
Edinburgh, UK
sbilbao@staffmail.ed.ac.uk

ABSTRACT

Finite difference time domain (FDTD) approaches to physical modeling sound synthesis, though more computationally intensive than other techniques (such as, e.g., digital waveguides), offer a great deal of flexibility in approaching some of the more interesting real-world features of musical instruments. One such case, that of brass instruments, including a set of time-varying valve components, will be approached here using such methods. After a full description of the model, including the resonator, and incorporating viscothermal loss, bell radiation, a simple lip model, and time varying valves, FDTD methods are introduced. Simulations of various characteristic features of valve instruments, including half-valve impedances, note transitions, and characteristic multiphonic timbres are presented, as are illustrative sound examples.

1. INTRODUCTION

The brass family is probably the most studied, among all the musical instruments, from the perspective of pure musical acoustics, and a full list of references would be quite long; for a general overview of the state of the art in brass instrument physics, see [1, 2].

Sound synthesis through physical modeling has developed along various lines; some formulations are based around the now-standard time-domain picture of the brass instrument as a nonlinear excitation coupled to a linear resonator [3], where the tube itself is characterized by its reflection function—among such methods are digital waveguides [4]. If wave propagation is consolidated in delay lines, and if loss and dispersion effects are modelled as lumped, such methods can be extremely efficient. See [5] for recent work on methods related to the waveguide formalism.

Finite difference time domain methods [6], based on direct time/space discretization of the acoustic field, though not as efficient as such structures, allow a very general approach to bore modelling, in particular when more realistic features typical of such instruments are incorporated. One such feature, the action of the brass instrument valve, will be described here; as will be seen, though such effects, necessarily time varying, lead to complications in terms of algorithm design, the resulting computational structure, and associated computational costs, are altered little.

A model of a brass instrument, including a linear model of the bore, a simple excitation mechanism, and valve junctions is presented in Section 2, followed by a description of a simple FDTD scheme in Section 3. Simulation results are presented in Section 4. Synthetic sound examples, created in the Matlab environment, are available at

http://www2.ph.ed.ac.uk/~sbilbao/brasspage.htm

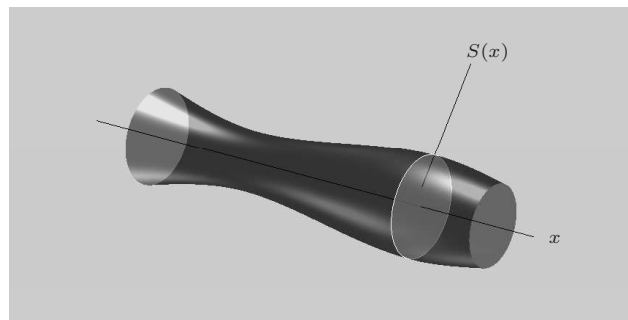

Figure 1: *An acoustic tube, of cross-section $S(x)$.*

2. BRASS INSTRUMENT MODELS

2.1. Lossless Tubes

Lossless wave propagation in an acoustic tube of variable cross section is described by the following well-known pair of equations:

$$p_t + \frac{\rho c^2}{S}\left(Sv\right)_x = 0 \tag{1a}$$

$$v_t + \frac{1}{\rho}p_x = 0 \tag{1b}$$

Here, $p(x,t)$ and $v(x,t)$ are the pressure deviation (from atmospheric) and particle velocity, respectively, at coordinates $x \in [0, L]$ and $t \geq 0$ along a tube of length L m. Subscripts x and t indicate partial differentiation with respect to a spatial coordinate and time, respectively. $S(x)$ is the surface area of the tube at location x, ρ is the density of air, in kg/m^3 and c is the speed of sound, in m/s.

When combined into a single second order equation in p, Webster's equation [7] results. In the interest of keeping the door open to the simulation of distributed nonlinear wave propagation (see [8]), the first order system above will be retained here. Webster's equation, and its variants, are the starting point for physical modeling sound synthesis both in speech [9], including the well-known Kelly-Lochbaum model [10] as well as in brass instruments [11]. The coordinate x will here be taken to be distance along the bore axis—see Figure 1; in a more refined model, it could represent a coordinate normal to isophase surfaces of one-parameter waves, for which there are many choices (see [12]), but the system above remains of essentially the same form.

In this article, since the final structure will be composed of a number of interconnected tubes, system (1) above represents wave

propagation in a single such tube, of length L.

2.2. Lip Model

It is not the purpose of this paper to investigate lip models, which have seen a great deal of theoretical work—see, e.g., [2] for an overview. A standard model is of the following form:

$$\frac{d^2y}{dt^2} + g\frac{dy}{dt} + \omega^2(y - H) = \frac{S_r \Delta p}{\mu} \tag{2}$$

In this simple model, the lip displacement $y(t)$, is modelled in terms of a single mass/spring/damper system, driven by a pressure difference Δp across the lips, defined as

$$\Delta p = p_m - p(0, t) \tag{3}$$

where $p_m(t)$ is the blowing pressure, and where $p(0, t)$ is the pressure at the entrance to a tube, the behaviour of which is defined by (1). ω is the angular lip frequency (a control parameter) , g is a loss coefficient, and μ is the lip mass (which is sometimes modelled as frequency dependent in the case of lip reed models [13, 14]). S_r is the effective surface area of the lips, and H is an equilibrium opening distance. Further closing relations are

$$u_m = wy\sqrt{\frac{2|\Delta p|}{\rho}}\mathrm{sign}(\Delta p) \tag{4a}$$

$$u_r = S_r\frac{dy}{dt} \tag{4b}$$

$$S(0)v(0, t) = u_m + u_r \tag{4c}$$

where u_m is volume flow at the mouth, u_r is flow induced by the motion of the lips, and where w is the channel width.

The model above is sometimes simplified by assuming $u_r = 0$ [2], or extended through the incorporation of an inertia term [13]; other varieties, including more degrees of freedom for lip motion are also available [14].

2.3. Bell Radiation

A simple model for radiation at the bell, relating particle velocity $v(x = L, t)$ and $p(x = L, t)$ is of the following form:

$$Z_c v = \alpha_1 p + \alpha_2 m \qquad p = \frac{dm}{dt} \tag{5}$$

where the parameters α_1 and α_2, and the characteristic impedance Z_c are defined by

$$\alpha_1 = \frac{1}{4(0.6133^2)} \quad \alpha_2 = \frac{c}{0.6133r} \quad Z_c = \rho c \tag{6}$$

where r is the radius of the bell opening. $m = m(t)$ is an extra lumped variable, reflecting the reactive character of the boundary condition. Such a condition corresponds to a rational (and positive real) approximation to the impedance of an unflanged tube. Such rational approximations are used frequently in speech synthesis [9]; this particular crude approximation matches fairly well with more refined approximations used in brass instrument models [15], and could be improved significantly using a higher order rational approximation [16](with the important constraint that positive realness is preserved).

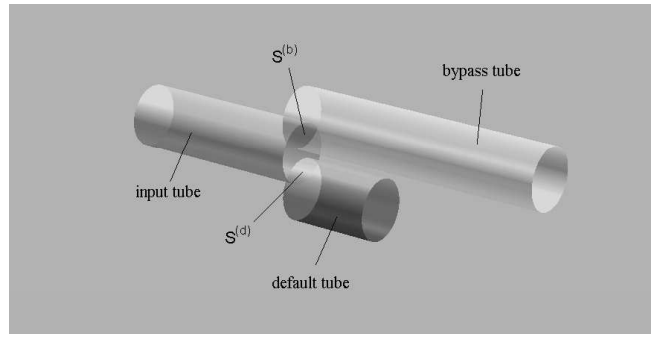

Figure 2: *Representation of a junction between an input tube, a default section of tube and a bypass section.*

2.4. Valve Junctions

A valve in a brass instrument allows for changes in the effective length of an instrument, through the introduction of an alternate length of tubing. In the most general case of a partly open valve, wave propagation is thus possible both through a short default section of tubing, and a bypass section.

Consider a junction of three tubes, as illustrated in Figure 2. Assuming lossless flow, the pressures at the junction in all three tubes are assumed equal, i.e.,

$$p^{(in)} = p^{(d)} = p^{(b)} \tag{7}$$

where the superscripts (in), (d) and (b) refer to the input, default and bypass sections, resepctively. The volume velocities sum to zero, i.e.,

$$S^{(in)}v^{(in)} = S^{(d)}v^{(d)} + S^{(b)}v^{(b)} \tag{8}$$

where $S^{(in)}$ is the surface area of the input tube at the junction, and where $S^{(d)}$ and $S^{(b)}$ are the overlapping surface areas of the tubes at the junction. For consistency, $v^{(in)}$ is positive when flow is in the direction of the junction, and $v^{(d)}$ and $v^{(b)}$ are negative.

$S^{(d)}$ and $S^{(b)}$ are dependent on the valve state. Because, in either the fully open or closed state, there is not a sizeable discontinuity in the tube cross section, it is useful to parameterize these areas as

$$S^{(d)} = q^{(d)}S^{(in)} \qquad S^{(b)} = q^{(b)}S_{(in)} \tag{9}$$

for given values $q^{(d)}(t)$ and $q^{(b)}(t)$, which depend on the current state of the valve at time t. When the tube valve is undepressed, $q^{(d)} = 1$ and $q^{(b)} = 0$, and when depressed, $q^{(d)} = 0$ and $q^{(b)} = 1$.

For a multivalve instrument, then, a single valve is characterised by its location along the bore, the lengths of the default and bypass tubes and its valve state. It can be assumed that the region of the instrument over which the valves are placed is cylindrical, as is the bypass tube, but this is by no means necessary in the FDTD framework.

2.5. Viscothermal Losses

Boundary layer effects in the horn lead to losses which may not be neglected, as they dominate bell radiation losses over the range of playing frequencies for a typical brass instrument—and have a great effect on the impedance curve for the instrument, and thus its playability. They are usually modelled in the frequency domain

through a transmission line formulation (see, e.g., [17, 15], for two slightly different models), and, when converted to the time/space domain, lead to a form similar to (1), but involving new terms:

$$p_t + \frac{\rho c^2}{S}\left(Sv\right)_x + f p_{t\frac{1}{2}} = 0 \quad (10a)$$

$$v_t + \frac{1}{\rho} p_x + g v_{t\frac{1}{2}} = 0 \quad (10b)$$

Here, fractional derivative terms have appeared—the accompanying spatially-varying coefficients are

$$f(x) = 2(\alpha - 1)\sqrt{\frac{\eta\pi}{\nu\rho S(x)}} \quad g(x) = 2\sqrt{\frac{\eta\pi}{\rho S(x)}} \quad (11)$$

Here, α is the ratio of specific heats for air, ν is the Prandtl number, and η is the shear viscosity coefficient. See [17] for precise values for these constants. Higher order terms (which play a role only for very thin acoustic tubes) have been neglected here; under further simplification, and after the reduction of the system above to a single second order equation (in p), a form similar to the Webster-Lokshin equation results [18]; the Webster-Lokshin formulation has been used previously in a brass sound synthesis framework [5].

3. FDTD SCHEMES

3.1. Simple Scheme for the Lossless System

System (1) is of the form of a pair of variable transmission line equations (or telegrapher equations [19]), and as such, is analogous to 1D electromagnetic wave propagation, the usual starting point for FDTD methods [20, 21]). An interleaved scheme of the form

$$p_l^n - p_l^{n-1} + \frac{\lambda Z_c}{\bar{S}_l}\left(S_{l+\frac{1}{2}} v_{l+\frac{1}{2}}^{n-\frac{1}{2}} - S_{l-\frac{1}{2}} v_{l-\frac{1}{2}}^{n-\frac{1}{2}}\right) = 0 \quad (12a)$$

$$v_{l+\frac{1}{2}}^{n+\frac{1}{2}} - v_{l+\frac{1}{2}}^{n-\frac{1}{2}} + \frac{\lambda}{Z_c}\left(p_{l+1}^n - p_{l-1}^n\right) = 0 \quad (12b)$$

is appropriate. p_l^n is an approximation to $p(x,t)$ at $x = lh$, and $t = nk$, for integer n and l, and for a grid spacing h and time step k; $f_s = 1/k$ is the sample rate. Similarly, $v_{l+\frac{1}{2}}^{n+\frac{1}{2}}$ is an approximation to $v(x,t)$ at $x = (l+\frac{1}{2})h$, and $t = (n+\frac{1}{2})k$, again for integer n and l. The functions $S_{l+\frac{1}{2}}$ and $\bar{S}_l$ are approximations to $S(x)$ and $x = (l+\frac{1}{2})h$ and $x = lh$, respectively. The characteristic impedance Z_c is as defined in (6), and the numerical parameter λ, or the Courant number [6] is defined as

$$\lambda = ck/h \quad (13)$$

It is possible to show, using either frequency domain or energy techniques [22] that a necessary stability condition for the scheme, if $\bar{S}_l$ is chosen as $\bar{S}_l = (S_{l+\frac{1}{2}} + S_{l-\frac{1}{2}})/2$, is

$$\lambda \leq 1 \qquad \rightarrow \qquad h \geq ck \quad (14)$$

Generally, it is best to choose h, given k (fixed by the sample rate, which is chosen a priori) as close to this bound as possible, to minimize numerical dispersion, and maximize output bandwidth. See [8] for more on the subject of accuracy. In the special case that $\lambda = 1$, the system above becomes equivalent, upon the introduction of wave variables, to the Kelly-Lochbaum model [10], and, furthermore, when S is constant, to a digital waveguide [4].

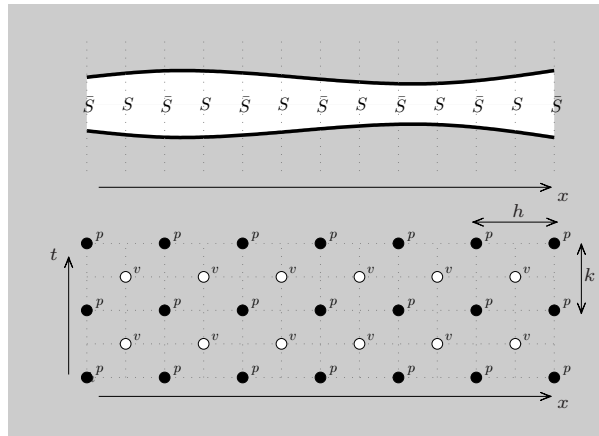

Figure 3: *Top: acoustic tube, for which approximations to the surface area S and $\bar{S}$ are made at alternating grid locations. Bottom: interleaved time/space grid for pressure p and velocity v.*

For a tube of length L, it is convenient (though by no means necessary) to choose h such that $N = L/h$ is an integer, while satisfying (14). In this case, p_l^n runs over integers $l = 0, \ldots, N$, taking on values at the endpoints of the tube, and $v_{l+\frac{1}{2}}^{n-\frac{1}{2}}$ at the interleaved values, from $l = 0, \ldots, N-1$. One implication of such a choice, in a network composed of many such tubes (such as a brass instrument) is that one will have a different grid spacing, and associated value of the Courant number λ for each tube segment.

3.2. Termination Conditions

Discretization of the termination conditions is similar to the case of reed wind instruments, discussed in [22], and is reviewed only briefly here.

At the bell termination of the final tube segment, the update is

$$p_N^n - p_N^{n-1} + \frac{\lambda Z_c}{\bar{S}_N}\left(S_{N+\frac{1}{2}} v_{N+\frac{1}{2}}^{n-\frac{1}{2}} - S_{N-\frac{1}{2}} v_{N-\frac{1}{2}}^{n-\frac{1}{2}}\right) = 0 \quad (15)$$

which requires access to the virtual value $v_{N+\frac{1}{2}}^{n-\frac{1}{2}}$. An approximation to the radiation boundary condition (5), namely

$$v_{N+\frac{1}{2}}^{n-\frac{1}{2}} + v_{N-\frac{1}{2}}^{n-\frac{1}{2}} = \frac{\alpha_1}{Z_c}\left(p_N^n + p_N^{n-1}\right) + \frac{\alpha_2}{Z_c}\left(m^n + m^{n-1}\right)$$

$$p_N^n + p_N^{n-1} = \frac{2}{k}\left(m^n - m^{n-1}\right)$$

allows the closure of the system, where an extra update in a time series $m = m^n$ is required. The above boundary condition may be shown to be numerically passive [22], and thus there is no risk of numerical instability.

For the lip model, the various dependent variables may be replaced by time series, i.e., $y^n, \Delta p^n, u_m^{n+\frac{1}{2}}, u_r^{n+\frac{1}{2}}$, approximating the various functions at interleaved multiples of k, the time step. The only time-dependent equations are (2) and (4b), which may be

approximated directly as

$$\frac{1}{k^2}\left(y^{n+1}-2y^n+y^{n-1}\right) \quad + \quad \frac{g}{2k}\left(y^{n+1}-y^{n-1}\right)$$
$$+\frac{\omega^2}{2}\left(y^{n+1}+y^{n-1}\right)-H=\frac{S_r\Delta p^n}{\mu} \tag{16}$$
$$u_r^{n+\frac{1}{2}} \quad = \quad \frac{S_r}{k}\left(y^{n+1}-y^n\right) \tag{17}$$

3.3. Tube Boundaries

Consider now a junction of three tubes, as described in Section 2.4. In the FDTD setting, with each of the schemes for the three tubes (impinging, default and bypass) is associated a distinct Courant number $\lambda^{(in)}$, $\lambda^{(d)}$ and $\lambda^{(b)}$, all of which should be chosen as close to unity as possible. Furthermore, as pressure values calculated by the three schemes at the junction are coincident, it is straightforward to translate condition (7) to the discrete setting (suppressing time indeces), as

$$p_N^{(in)}=p_0^{(d)}=p_0^{(b)}=p^{(J)} \tag{18}$$

where $p^{(J),n}$ is the common pressure at the junction, and where $p_N^{(in),n}$ is the pressure in the impinging tube at its right end, and where $p_0^{(d),n}$ and $p_0^{(b),n}$ are the pressure in the default and bypass sections.

The updates (12a) require access to values of the velocity grid functions at virtual locations not on the respective grids, i.e., $v_{N+\frac{1}{2}}^{(in)}$, $v_{-\frac{1}{2}}^{(d)}$ and $v_{-\frac{1}{2}}^{(b)}$. These can be set according to the flow boundary condition (8) as

$$S_{N-\frac{1}{2}}^{(in)}v_{N-\frac{1}{2}}^{(in)}+S_{N+\frac{1}{2}}^{(in)}v_{N+\frac{1}{2}}^{(in)}= \tag{19}$$
$$S_{-\frac{1}{2}}^{(in)}v_{-\frac{1}{2}}^{(d)}+S_{\frac{1}{2}}^{(d)}v_{\frac{1}{2}}^{(d)}+S_{-\frac{1}{2}}^{(b)}v_{-\frac{1}{2}}^{(b)}+S_{\frac{1}{2}}^{(b)}v_{\frac{1}{2}}^{(b)}$$

The conditions (18) and (19) may be combined to give a single update for the junction pressure $p^{(J),n}$ as

$$p^{(J),n}-p^{(J),n-1}= \tag{20}$$
$$\beta^{(J)}\left(S_{N-\frac{1}{2}}^{(in)}v_{N-\frac{1}{2}}^{(in),n-\frac{1}{2}}-S_{\frac{1}{2}}^{(d)}v_{\frac{1}{2}}^{(d),n-\frac{1}{2}}-S_{\frac{1}{2}}^{(b)}v_{\frac{1}{2}}^{(b),n-\frac{1}{2}}\right)$$

where $\beta^{(J)}$ is given by

$$\beta^{(J)}=\frac{2Z_c}{S_N^{(in)}\left(1/\lambda^{(in)}+q^{(b)}/\lambda^{(b)}+q^{(d)}/\lambda^{(d)}\right)} \tag{21}$$

where $q^{(b)}$ and $q^{(d)}$ follow from the current valve state, as in (9).

The above explicit update for the junction pressure should suggest the analogous update in a scattering framework (such as wave digital filters [23] or digital waveguides [4]). Conversely, it may also be seen that the explicit updating, often claimed to be a benefit of such approaches, is in fact characteristic of direct (i.e., non-scattering) methods as well.

3.4. Filter Designs and Viscothermal Losses

The fractional derivative terms in (10), though standard in frequency domain analysis of acoustic tubes [15] pose some numerical challenges in the FDTD setting, as they do in scattering based approaches. A simple approach (among many; see [24, 5] for other examples) which has been described recently in [8], is to employ an FIR filter design. To approximate the term $p_{t^{\frac{1}{2}}}$ in (10a), one may employ, generally,

$$p_{t^{\frac{1}{2}}}(x,t)\approxeq\sum_{m=0}^{M}a_m p_l^{n-m} \tag{22}$$

for some suitably chosen parameters a_m (perhaps through a frequency domain optimization procedure), and for a chosen order M. In order to get reasonable accuracy at low frequencies, the order M must be chosen to be moderately high—between 20 and 40, at a typical audio sample rate, such as $f_s=44100$ Hz. A similar approximation may obviously be used for the term $v_{t^{\frac{1}{2}}}$ in (10b). Scheme (12) may thus be generalized to

$$p_l^n-p_l^{n-1} \quad + \quad \frac{\lambda Z_c}{S_l}\left(S_{l+\frac{1}{2}}v_{l+\frac{1}{2}}^{n-\frac{1}{2}}-S_{l-\frac{1}{2}}v_{l-\frac{1}{2}}^{n-\frac{1}{2}}\right)$$
$$+ \quad kf_l\sum_{m=0}^{M}a_m p_l^{n-m}=0 \tag{23a}$$
$$v_{l+\frac{1}{2}}^{n+\frac{1}{2}}-v_{l+\frac{1}{2}}^{n-\frac{1}{2}} \quad + \quad \frac{\lambda}{Z_c}\left(p_{l+1}^n-p_{l-1}^n\right)$$
$$+ \quad kg_{l+\frac{1}{2}}\sum_{m=0}^{M}a_m v_{l+\frac{1}{2}}^{n+\frac{1}{2}-m}=0 \tag{23b}$$

where f_l and $g_{l+\frac{1}{2}}$ are approximations to $f(x)$ and $g(x)$ from (11) at locations $x=lh$ and $x=(l+\frac{1}{2})h$, respectively.

It is important to point out that the order M of the approximation will determine the memory requirement for the algorithm as a whole, and has a strong impact on computational complexity—see Section 3.5. It would thus be advantageous to employ rational filter designs of potentially much lower order.

3.5. Computational Costs

The computational cost of the scheme for the entire system is determined by the total length of tube, L_{total}, which is made up of contributions from the main bore, as well as the bypass tubes. For a Courant number of 1 in all the sections (this is the worst case), the total number of grid points will be $N(f_s)=L_{total}f_s/c$, and thus the total memory requirement, to hold both pressure and velocity variables, will be

$$\text{memory requirement}=2NM \tag{24}$$

where M is the order of the approximating filter for viscothermal losses. The combined addition+multiplication count per second will be

$$\text{operation count/sec.}=N(4M+6)f_s \tag{25}$$

At $f_s=44100$, for a total tube length of $L=1$ m, and for $M=20$, the floating point operation rate is on the order of 500 Mflops. This is not cheap, compared with, e.g., a digital waveguide implementation, but neither is it exorbitant, by the standards of todays microprocessors. On the other hand, using such a scheme in a time-varying setting (i.e., employing valve transitions) requires only $O(1)$ additional operations per time step, and is thus of negligible cost.

4. SIMULATION RESULTS

In this section, simulation results are presented for a given bore profile corresponding to a Smith-Watkins trumpet, with a Kelly Screamer mouthpiece. The bore profile is shown in Figure 4. Valves are located at 67.3, 72 and 75 cm along the bore from the mouthpiece end, and the bypass tube lengths are 27 cm, 20 cm and 15 cm, respectively; the default tube lengths are all 2 cm.

4.1. Simulated Impedances

As a preliminary check of the validity of this method, a comparison between a measured input impedance curve for a trumpet, and one computed using an FDTD method, running at 44.1 kHz, is shown in Figure 4. The curves match well over most of the playing range of the instrument, with some deviations apparent above 1 kHz—these are due to the particular simple choice of radiation impedance made here, which underestimates loss at high frequencies, and which could be easily rectified by using a higher order rational approximation.

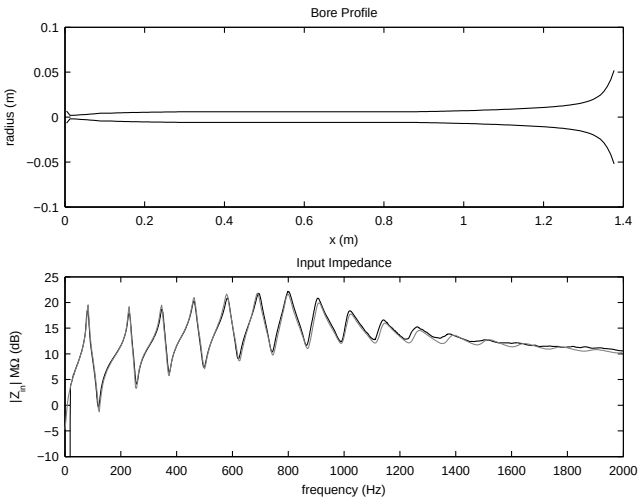

Figure 4: *Bore profile, top, for a trumpet, including the mouthpiece, and input impedance magnitudes, bottom, from measurement (black) and simulation (grey).*

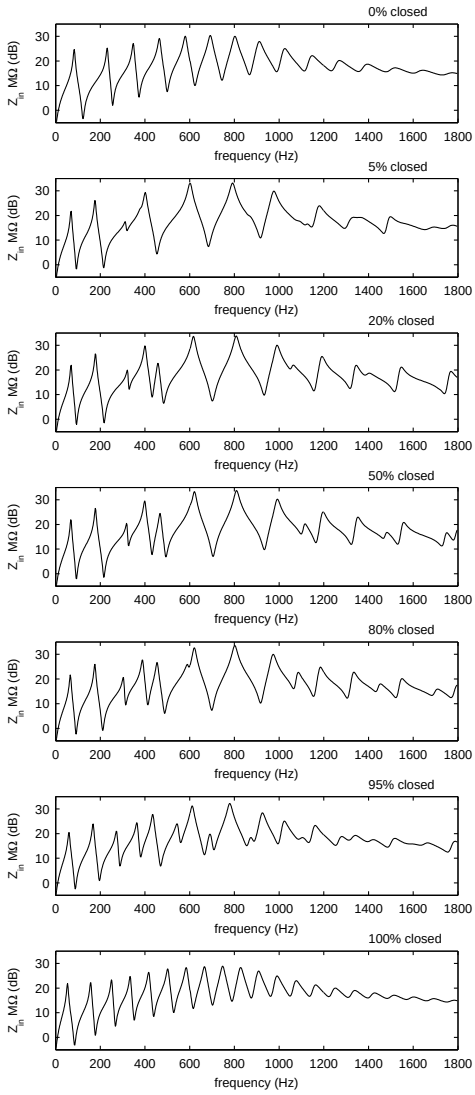

Figure 5: *Input impedance magnitudes, for a trumpet, under partially closed valve conditions. Successive plots show impedance magnitudes at varying degrees of simultaneous closure of all three valves (with 100% corresponding to a fully depressed state).*

4.2. Half-valve Impedances

As an example of the behaviour of this numerical method, it is interesting to examine simulated impedance curves, under different half-valve configurations, as illustrated in Figure 5.

4.3. Valve Transitions

In its simplest use, the system described here should be capable of effecting simple changes in pitch. See Figure 6 for a spectrogram of sound output when a single valve is depressed in the model, where the bore profile is that of a trumpet. In this case, the lip parameters and blowing pressure are kept constant, but in a true playing situation, however, one would expect that various parameters (and especially the blowing pressure and lip frequency) are varied simultaneously. Depending on the precise trajectories of these control signals, one expects a wide variety of possible note transitions, and also situations where the note transition does not occur, and there is rather a noise like timbre, warble, or multiphonic results—see Section 4.5.

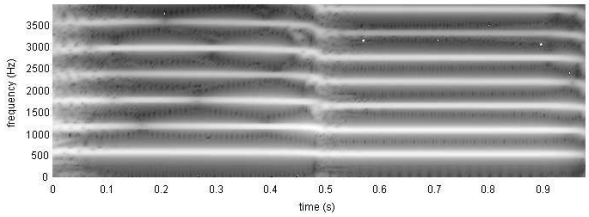

Figure 6: *Spectrogram of sound output for a typical valve transition, for a trumpet bore, with a single valve (effecting a change in pitch of a semitone).*

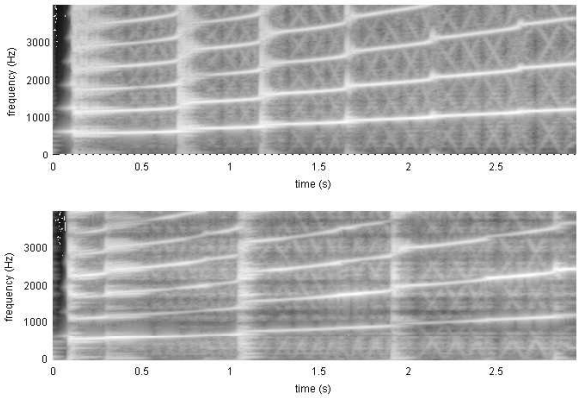

Figure 7: *Spectrogram of sound output under a constant linear sweep of the lip frequency, for a trumpet, when all valves are undepressed (top), and half depressed (bottom).*

4.4. Glissandi

From Figure 5, illustrating impedance curves under partially closed valve conditions, one may note that when all valves are approximately half open, the resonances over the middle of the playing range become more sparse, and are relatively wide. Under such conditions, a player may more easily effect a glissando than in the case when valves are all in an either fully depressed or undepressed state. See Figure 7, showing spectrograms illustrating a typical gesture under both conditions.

4.5. Warbles and Multiphonics

The irregularity of the impedance curve for an instrument with all valves partially depressed, leads to a wide variety of possible behaviours.

See Figure 8, showing spectrograms of sound output, for a trumpet with all valves half depressed, and for slightly different lip frequencies. At 320 Hz, the instrument produces a pure tone, at 350 Hz, a warble at a sub-audio rate, and at 400 Hz, a noise-like timbre. As can also be observed, note onset times vary considerably with frequency.

4.6. Sound Examples

Sound examples are available on the author's website at

`http://www2.ph.ed.ac.uk/~sbilbao/brasspage.htm`

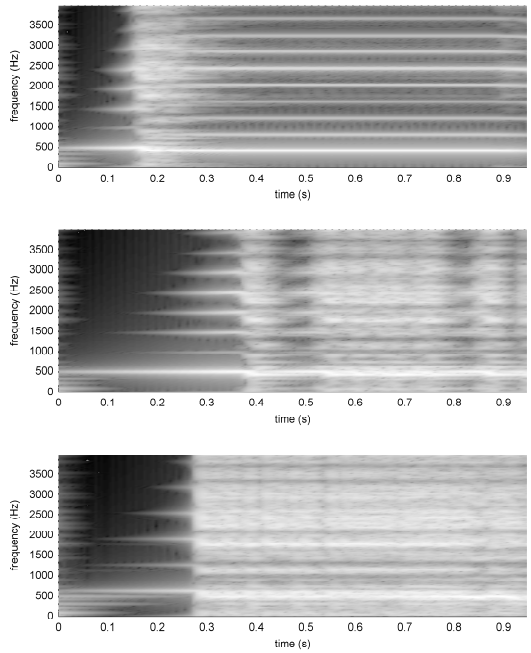

Figure 8: *Spectrograms of sound output, for a trumpet, when all valves are half depressed, under different lip frequencies. Top: 320 Hz, middle, 350 Hz and bottom, 400 Hz.*

5. CONCLUSIONS AND FUTURE WORK

At the level of the model itself, numerous refinements are possible, which do not alter the basic computational structure described here. Among these are a closer attention to the precise definition of Webster's equation (and an appropriate choice of spatial coordinate), as mentioned in Section 2.1, and an improved model of the radiation impedance, as described in Section 2.3; such refinements lead to relatively minor improvements, in terms of agreement between experiment and simulation (which is already quite good for the model presented here), and may not lead to any discerible benefits in synthesis.

The incorporation of nonlinear effects as described recently in [8], on the other hand, is anticipated to be of major perceptual significance, and requires a more involved treatment (perhaps resorting to finite volume methods [25], and employing artificial viscosity in order to prevent numerical oscillation near the formation of a shock front); even in this case, however, the basic structure of the scheme remains little changed.

As far as the scheme itself is concerned, though the lossless scheme (12) performs very well indeed, the discrete-time approximation to viscothermal losses is rather crude, and leads to a computational bottleneck, both in terms of memory and the over-all operation count. A better approach would perhaps be to use a rational filter approximation; while not problematic in the linear case, such IIR filters, when used to approximate viscothermal losses, will generally exhibit large variations in the coefficient values themselves, and may be difficult to employ in conjunction with a fully

nonlinear model of wave propagation.

Because the scheme is uniform over the entire length of the bore (i.e., grid points are treated equally, and there is not a decomposition into variable length components, or lumping of loss or dispersion effects), programming complexity is quite low for such methods; indeed, in the Matlab code written by the author, the update for the bore in the run time loop may be written in four lines. It is also very well suited to parallelization in a multicore or GPGPU environment.

One aspect of synthesis which has not been discussed here in any detail is that of control. The determination of lip parameters, such as frequency and mass, necessarily time varying, during a playing gesture already presents a difficult experimental challenge; when the extra layer of valve control is also present, the challenges become formidable. Such difficulties are to be expected in any complete physical modeling synthesis framework, and are, in many ways, a measure of the maturity of physical modeling synthesis—beyond building the instrument, one must also learn how to play it. It is thus hoped that the synthesis algorithm presented here will also be useful in scientific studies of brass instrument playing, and such work is under way at the University of Edinburgh.

6. ACKNOWLEDGMENTS

Thanks to Shona Logie, John Chick and Arnold Myers, at the University of Edinburgh, for providing measurements of bore profiles and impedance curves for various brass instruments.

7. REFERENCES

[1] A. Chaigne and J. Kergomard, *Acoustique des Instruments de Musique*, Belin, Paris, France, 2008.

[2] N. Fletcher and T. Rossing, *The Physics of Musical Instruments*, Springer-Verlag, New York, New York, 1991.

[3] M. McIntyre, R. Schumacher, and J. Woodhouse, "On the oscillations of musical instruments," *Journal of the Acoustical Society of America*, vol. 74, no. 5, pp. 1325–1345, 1983.

[4] J. O. Smith III, *Physical Audio Signal Procesing*, Stanford, CA, 2004, Draft version. Available online at `http://ccrma.stanford.edu/~jos/pasp04/`.

[5] R. Mignot and T. Hélie, "Acoustic modelling of a convex pipe adapted for digital waveguide simulation," in *Proceedings of the 13th International Digital Audio Effects Conference*, Graz, Austria, September 2010.

[6] J. Strikwerda, *Finite Difference Schemes and Partial Differential Equations*, Wadsworth and Brooks/Cole Advanced Books and Software, Pacific Grove, California, 1989.

[7] P. Morse and U. Ingard, *Theoretical Acoustics*, Princeton University Press, Princeton, New Jersey, 1968.

[8] S. Bilbao, "Time domain modelling of brass instruments," in *Proceedings of Forum Acusticum*.

[9] L. Rabiner and R. Schafer, *Digital Processing of Speech Signals*, Prentice-Hall, Englewood Cliffs, New Jersey, 1978.

[10] J. Kelly and C. Lochbaum, "Speech synthesis," in *Proceedings of the Fourth International Congress on Acoustics*, Copenhagen, Denmark, 1962, pp. 1–4, Paper G42.

[11] D. Berners, *Acoustics and Signal Processing Techniques for Physical Modelling of Brass Instruments*, Ph.D. thesis, Department of Electrical Engineering, Stanford University, 1999.

[12] T. Hélie, "Unidimensional models of acoustic propagation in axisymmetric waveguides," *Journal of the Acoustical Society of America*, vol. 114, no. 5, pp. 2633–2647, 2003.

[13] D. Keefe, "Physical modeling of wind instruments," *Computer Music Journal*, vol. 16, no. 4, pp. 57–73, 1992.

[14] S. Adachi and M. Sato, "Time-domain simulation of sound production in the brass instrument," *Journal of the Acoustical Society of America*, vol. 97, no. 6, pp. 3850–3861, 1995.

[15] R. Caussé, J. Kergomard, and X. Lurton, "Input impedance of brass musical instruments—comparison between experiment and numerical models," *Journal of the Acoustical Society of America*, vol. 75, no. 1, pp. 241–254, 1984.

[16] F. Silva, P. Guillemain, J. Kergomard, B. Mallaroni, and A. Norris, "Approximation forms for the acoustic radiation impedance of a cylindrical pipe," *Journal of Sound and Vibration*, vol. 322, pp. 255–263, 2009.

[17] D. Keefe, "Acoustical wave propagation in cylindrical ducts: Transmission line parameter approximations for isothermal and nonisothermal boundary conditions," *Journal of the Acoustical Society of America*, vol. 75, no. 1, pp. 58–62, 1984.

[18] T. Hélie and D. Matignon, "Diffusive representations for the analysis and simulation of flared acoustic pipes with viscothermal losses," *Mathematical Models and Methods in Applied Sciences*, vol. 16, no. 4, pp. 503–536, 2006.

[19] D. Cheng, *Field and Wave Electromagnetics*, Addison-Wesley, Reading, Massachusetts, second edition, 1989.

[20] A. Taflove, *Computational Electrodynamics*, Artech House, Boston, Massachusetts, 1995.

[21] K. Yee, "Numerical solution of initial boundary value problems involving Maxwell's equations in isotropic media," *IEEE Transactions on Antennas and Propagation*, vol. 14, pp. 302–307, 1966.

[22] S. Bilbao, *Numerical Sound Synthesis: Finite Difference Schemes and Simulation in Musical Acoustics*, John Wiley and Sons, Chichester, UK, 2009.

[23] A. Fettweis, "Wave digital filters: Theory and practice," *Proceedings of the IEEE*, vol. 74, no. 2, pp. 270–327, 1986.

[24] J. Abel, T. Smyth, and J. O. Smith III, "A simple, accurate wall loss filter for acoustic tubes," in *Proceedings of the 6th International Digital Audio Effects Conference*, London, UK, September 2003, pp. 254–258.

[25] R. Leveque, *Finite Volume Methods for Hyperbolic Problems*, Campbridge University Press, Cambridge, UK, 2002.